Bulletin of the Seismological Society of America, Vol. 94, No. 3, pp. 818–827, June 2004

Ⓔ

# Source Parameters and Tectonic Implications of Aftershocks of the $M_w$ 7.6 Bhuj Earthquake of 26 January 2001

by Paul Bodin and Steve Horton

Abstract We present and discuss the spatial distribution of more than 1000 aftershocks of the largest continental intraplate earthquake to occur during the modern seismological period. The data were recorded on a network of eight portable digital seismographs deployed for 3 weeks starting 17 days after the mainshock. We have calculated high-quality single-event locations, based on a 1D velocity model determined for the region for earthquakes with magnitudes between ~2 and 5. Aftershock locations reveal activity concentrated on a nearly east-striking, south-dipping plane, trapezoidal in outline. The active zone tapers from about 45 km along strike at the shallow end, which is about 5 km deep, to no more than 25 km long at a depth of 35 km. The total rupture area was about 1300 km$^2$. We estimate the static stress drop of the mainshock at 16 ± 2 MPa. Aftershocks extend nearly through the entire crust, with concentrations in the lower crust at about 26 km and in the upper crust at about 10 km. The fault that ruptured was not mapped at the surface and not known to have been active prior to the 2001 earthquake. The aftershock data are consistent with the Bhuj earthquake resulting from reactivation in contraction of a fault formed under extension within a failed rift.

*Online material:* Source parameters of recorded Bhuj aftershocks.

## Introduction

The $M_w$ 7.6 Bhuj earthquake occurred on the morning of 26 January 2001 in Gujarat, India, as an unprepared community readied Republic Day celebrations. The death toll from the earthquake exceeded 20,000, and the event resulted in widespread collapse of or damage to poorly engineered structures. The Bhuj earthquake was the largest earthquake in the region since the $M_w$ ~7.8 Rann of Kachchh (also spelled Kutch, Kuch, Cutch, and other variants) earthquake of 1819 and the largest continental-intraplate earthquake globally in more than 100 years. Understanding its source properties presents the opportunity to enhance our understanding of the mechanics of a rare class of earthquakes, at the same time clarifying its role in the active seismoteconic deformation of Kachchh. Its importance to global seismic hazard studies extends beyond northwestern India because it may be an analog for other continental intraplate earthquakes, particularly the New Madrid seismic zone in the central United States.

The Bhuj earthquake occurred in a poorly instrumented region, and as a result, much information that we associate with recent large earthquakes is unavailable. For example, the network of geodetic monuments in the region was sparse and not measured using the Global Positioning System (GPS); there were no strong ground motion recorders in the mesoseismal area, and the nearest on-scale regional broadband recording was at a distance of 550 km; and interferometric radar images are not of sufficient quality to develop a deformation picture. Moreover, all searches for surface breaks, impeded by difficult access and working conditions, have turned up no unequivocal evidence of primary rupture (Wesnousky *et al.*, 2001). So our tools to study this earthquake are the global seismic networks and remote regional seismic data, felt and damage reports, and studies of its aftershocks.

The earthquake focal mechanism derived from teleseismic observations indicates reverse faulting with nodal planes striking about east–west and dipping north and south (e.g., Harvard Centroid Moment Tensor [CMT] Catalog; Antolik and Dreger, 2003). This is consistent with north–south contraction within the Indian Plate. The source time function (STF) inferred from finite fault models of teleseismic observations (Antolik and Dreger, 2003, Singh *et al.*, 2003) was of a large simple pulse approximately 10 sec in duration followed, after a few-second hiatus, by a much smaller 10-sec-long moment-release pulse. The teleseismic modeling suggests that most of the moment was released from a relatively small fault area, with high slip (>12 m) and high stress drop (~20 MPa). Ground motion generated by the earth-

quake was felt 2000 km from the epicenter and caused light damage at sediment sites as far as 600 km away (Bendick *et al.*, 2001; Hough *et al.*, 2002). This is consistent with low crustal attenuation in the Indian shield and/or unusually high stress drop for earthquakes in India (e.g., Singh *et al.*, 1999a). However, the lack of surface rupture precluded the identification of the causative fault or many rupture details.

In this article, we present results and pertinent details about aftershocks recorded by a temporary seismic network we deployed in the epicentral region. We recorded more than 2000 events during the 18-day deployment, starting about 2.5 weeks after the mainshock. This deployment represents a cooperative effort between the Center for Earthquake Research and Information (CERI) at the University of Memphis, the Mid-America Earthquake Center (MAEC), and the Institute of Science and Technology Advanced Studies and Research (ISTAR). We have located a subset of the aftershocks, obtained a reasonable velocity model for the region, and generated first motion focal mechanisms. This work allows us to constrain the fault dimensions and orientation of the mainshock. We obtain an estimate of the static stress drop of the mainshock using the seismic moment independently estimated from teleseismic recordings. This is an important parameter for estimating ground-motion attenuation in intraplate regions. Finally, we discuss the tectonic setting of the Bhuj earthquake and its implications for seismic hazard in the region and in the eastern United States.

## Geologic and Tectonic Setting of the Bhuj Earthquake

The Bhuj earthquake occurred in the Kachchh rift, an intraplate region of rifted Precambrian craton in northwestern India. The rift is bounded by the Nagar Parker fault in the north and the Kathiawar fault in the south (Fig. 1). Precambrian granitic basement is exposed in the Nagar Parkar Hills bordering the northern flank of the rift graben (Biswas, 1987). The Kachchh rift is thought to have opened up along major Precambrian trends in the Early Jurassic, and the basin is filled with sediments ranging in age from Middle Jurassic to Holocene that overlie the Precambrian basement (Biswas, 1982). At the Banni deep well (northwest of the epicentral area), Precambrian granite porphyry/rhyolite is found at a depth of 1718.5 m (Singh, 1995).

Following rifting in the Early Jurassic, deposition of sediments occurred in sublittoral to deltaic sedimentary environments through the Lower Cretaceous (Biswas, 1981). Beginning in Late Cretaceous–Early Paleocene time, the Kachchh rift was again subjected to deformation. Around 66 Ma the Deccan/Reunion hot spot erupted (Courtillot *et al.*, 1986) and the western margin of India passed over the hot spot (Biswas, 1982). This event coincided with the onset of the collision of India with the southern margin of Eurasia from ~50 Ma (Besse *et al.*, 1984; Patriat and Achache, 1984) to ~66 Ma (Jaeger *et al.*, 1989; Beck *et al.*, 1995). Deformation within the rift appears to have been substantial at first, resulting in highly folded, faulted, and intruded Mesozoic strata, but it decreased through time as the Tertiary strata dip only gently (Biswas, 1982). By the Late Miocene (~20 Ma), the east–west–trending Kachchh Rift Basin was being subjected to an approximately north–south compressive stress field (Talwani and Gangopadhyay, 2001).

Highlands within the Kachchh rift expose Mesozoic strata and are surrounded by plains where younger sediments overlie the Mesozoic units. The uplifts are oriented generally east/west, and they tend to have escarpments facing the plains that Biswas (1980) suggested are the master faults of the uplifts. The three principal uplifts within the rift are the Kachchh Mainland, the Wagad uplift, and the Island Belt. The associated escarpments (faults) have these names.

The highlands are separated by subbasins in the form of half-grabens (Biswas, 1987). The subbasins are broad, gentle bowls of unconsolidated Tertiary and Holocene nearshore marine and fluvial sediment, known as Ranns. The Great Rann of Kachchh and the Little Rann are sea level salt wastes that are inundated during the monsoon with marine waters and terrestrial water runoff. Several hundred years ago, the Great Rann was apparently inundated by the sea deeply enough to permit rather large seagoing vessels to sail what is now quite far inland (Siveright, 1907; Talwani and Gangopadhyay, 2001). The north and south margins of the Rann are slightly (several meters at most) uplifted landscapes called the Banni (in the south) or the Bet (in the north). Bet and Banni sediments are not currently inundated by the sea, are composed largely of wind-blown silt that appears distinct in aerial images, and sustain some plant and animal life.

The level of current activity on the principal faults of the Kachchh rift is not clear. The two rift boundary faults (the Nagar Parkar and the Kathiawar) may not have been active since the Early Jurassic given that the top of the granitic basement is still deeper within the rift than outside. The three principal surface faults interior to the rift boundary (the Island Belt fault, the Kachchh Mainland fault, and the South Wagad fault) are clearly associated with the major topographic features within the Kachchh rift and have been active since the Mesozoic, since Mesozoic rocks are displaced along these features. However, the Tertiary strata within the subbasins are relatively undeformed, suggesting activity during the Tertiary has been minimal. Geologic and tectonic studies have also mapped several northeast- and northwest-striking faults in Kachchh that cut across the dominant east–west grain of the landscape (e.g., Malik *et al.*, 2000). The activity level of these faults is also unclear. Despite their prominence on tectonic maps and as surface features, none of the aforementioned faults was responsible for the 2001 Bhuj earthquake.

The Bhuj earthquake occurred 300–400 km from a recognized plate boundary (Fig. 1). West of Kachchh, a triple junction joins the Owen fracture zone (sinestral slip between the Indian and Arabian plates), the Chaman transform (sinistral slip between the Indian and Eurasian plates, with geological evidence of thrust faulting), and the eastern limit of

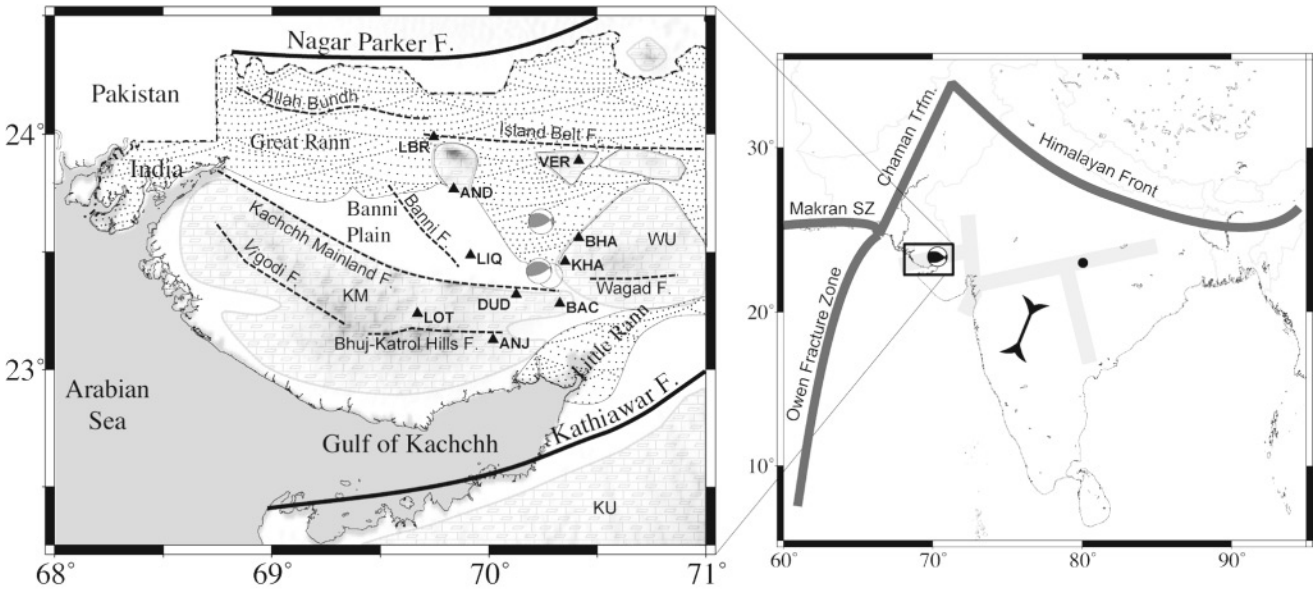


Figure 1. Tectonic setting of the Bhuj earthquake. Right: regional setting; the plate boundaries named in text are illustrated by wide dark gray lines, and the location of rift systems is schematically illustrated by wide light gray straight lines. The location of the 2001 Bhuj earthquake is indicated with focal mechanism. The black circle is the location of the 1997 Jabalpur earthquake. The black line represents the direction of the geodetically observed contraction of peninsular India, with rates between 1 and 5 mm/yr. Left: The Kachchh rift. Bold dark lines are rift bounding faults, other mapped faults are dashed. Uplifts are shown by block pattern: KU, Kathiawar uplift; WU, Wagad uplift, KM, Kachchh Mainland (smaller uplifts are unnamed). Rann areas are shown by stippled pattern. The black triangles are locations of CERI/MAEC/ISTAR temporary seismic stations, with station codes. Station LOT is within the principal city of the region, Bhuj. Focal mechanisms include the Harvard CMT (northernmost), the USGS fault-plane solution, and an open circle representing the epicenter as reported by the IMD.

the Makran convergent zone between the Arabian and Eurasian plates. Seismicity associated with these boundaries is rather diffuse, and much about the regional tectonics remains to be clarified. The Kachchh rift is being subjected to north-northeast-oriented compressional stress (Gowd *et al.*, 1992) reflecting contraction within the Indian plate of rates geodetically estimated to be from 1 to 10 mm/yr (Bilham and Gaur, 2000; Bilham *et al.*, 2002).

Background seismicity is apparently rather low, although seismic monitoring is for all practical purposes nonexistent. For example, only 24 earthquakes appear in the catalog of Malik *et al.* (1999) since the 1819 Allah Band earthquake, and the U.S. Geological Survey (USGS) Preliminary Determination of Epicenter (PDE) lists 19 instrumentally located earthquakes ($3.7 \leq m_b \leq 5.2$) since 1975 prior to the Bhuj earthquakes. Of course, the region is poorly instrumented and the background seismicity rate and characteristics are poorly constrained. The only seismic station in the region, at Bhuj, has been in operation for only a few years; the data are not generally available to assess regional background microsesimicity rates; and the record of the mainshock was clipped. Rajendran and Rajendran (2001) suggested only low levels of seismicity in the region. The largest recent earthquake was the $M$ 6.1 Anjar earthquake in 1956. This earthquake was apparently a shallow reverse rupture (Chung and Gao, 1995) but did not rupture the surface. On 24 December, 2001, an $M$ 5 earthquake struck north of Bhuj; the teleseismically determined epicenter is close to the western end of the Island Belt fault.

At the northwest edge of the Great Rann, the Allah Band, or Dam (wall) of God, was thrown up during the 1819 Great Rann of Kachchh earthquake ($M_w \sim 7.8$). A possible recurrence of this earthquake has dominated the perceived seismic hazard in the area. The 1819 earthquake rupture apparently did not reach cleanly to the surface, but rather was manifest as a monoclinal fold (Rajendran and Rajendran, 2001). Geodetic and geologic data have been interpreted as evidence that the 1819 rupture was on a shallow-dipping (to the north) fault. Paleoseismic studies suggest at least one and maybe two prior earthquakes (Rajendran and Rajendran, 2001).

## Aftershock Seismic Observations

### Seismic Instrumentation and Data Characteristics

We deployed eight Kinemetrics K2 digital recorders near the mainshock epicenter between 12 and 28 February

2001. Each K2 included an internal triaxial force-balance accelerometer set to full scale of 2*g* and a built-in GPS timing system. An external velocity sensor (Mark Products triaxial L-28) was also attached to each K2 to ensure detection of weak ground motion. All six channels were recorded at 200 samples per second. An external battery and solar panel provided power. Each K2 was operated in a Short Term Average/Long Term Average (STA/LTA) triggered mode with a trigger ratio of 4 on all channels. Pre-event time was 10 sec, and post-event time was 20 sec.

The eight-station network was designed primarily for aftershock location. Station coordinates are given in Table 1. Figure 1 shows the location of stations and two estimates of the mainshock epicenter. The general intent was to surround the area of aftershock activity. The network configuration was moderately impacted by logistical constraints imposed by the location of our base of operations in Bhuj and by the local road system. Travel time limited the extension of the network to the east. Available roads limited access to northern and central areas.

Most stations were sited on rock (sandstone or basalt) or on a thin layer of soil overlying rock. Station LIQ is a notable exception. Intentionally located at the site of a large sand-blow, the thickness of unconsolidated sediment at LIQ is thought to be around 500 m. The thickness of the soil layer at KHA and DUD is unknown.

The largest aftershock that we recorded was $m_b$ 5.2 (PDE), and several were $m_b > 4.0$. The largest acceleration recorded by our network was 108.8 cm/sec$^2$ (0.11*g*) at a station 20 km from an $m_b$ 4.7 earthquake.

Local aftershock monitoring was also carried out by the India Meteorological Department (IMD), the Geological Survey of India, the Indian National Geophysical Research Institute, and Hirosaki University, Japan (Negishi *et al.*, 2002). Because of communications difficulties before and during these field operations, all field operations were conducted independently and without knowledge of each other.

## Data Handling and Analysis

In this article, we present results from a standard analysis of single-event locations based on *P*- and *S*-wave arrival times. Event data were initially recorded on an internal 182 MB memory card. Each site was visited about every 48 hr to transfer data to a PC. Data were written to CD for storage and transportation to the United States, where the waveform data were converted into *miniseed* format for incorporation into the Incorporated Research Institutions in Seismology (IRIS) data management system. Events were declared when at least four stations triggered within a 30-sec window. More than 2000 events satisfied these criteria. We picked *P*- and *S*-wave arrival times, polarities, phase amplitudes, and signal durations on raw data files. Filtered (1-Hz low-passed) data were used to verify or modify arrival times. Phase arrivals were weighted by the picking uncertainty. Several analysts participated in phase picking, and care was taken to ensure that pick criteria were uniform and standardized.

We estimated hypocentral locations using the program HYPOELLIPSE (Lahr, 1999) and a velocity model with the shallow structure constrained by local geological and geophysical observations and the deeper structure constrained using travel-time observations of the aftershocks and ray theory (Horton *et al.*, 2001). A prominent feature of many seismograms we recorded was the presence of converted *S* waves to *P* waves at most stations within the network. The conversion is indicated by large phases on the vertical-component seismograms that arrive before the *S* phase on the horizontal seismograms. The time difference between these arrivals, $\Delta t$, varies around the network. The converted phases strongly indicate a low-velocity layer overlying a faster layer near the surface. We believe that the conversion occurs at the Precambrian to Mesozoic boundary, between 0.5 and 2.5 km below the surface across the network. From surface wave dispersion analysis (C. A. Langston, personal comm., 2003), we estimate the average *P*-wave velocity of the Mesozoic sediments to be 3.0 km/sec. Assuming an average thickness of Mesozoic and younger sediments of 1.5 km, and an average $\Delta t$ to be 0.75/sec, suggests an *S*-wave velocity of around 1.2 km/sec. We have only used the converted phase observations in a general way, to constrain an average 1D model. Deviations of individual stations from this average model were accounted for using station correc-

Table 1
Station Coordinates, Travel-Time Corrections, and Site Conditions

| Station | Latitude (°N) | Longitude (°E) | *P* Correction (sec) | *S* Correction (sec) | Site Conditions | |
|---|---|---|---|---|---|---|
| | | | | | Geology | Structures |
| AND | 23.7673 | 69.8388 | | | Sandstone | Stick hut |
| ANJ | 23.1278 | 70.0205 | 0.04 | 0.14 | Deeply weathered sandstone | Very small shed |
| BAC | 23.2807 | 70.3267 | −0.02 | −0.01 | Basalt flow | Free field |
| BHA | 23.5600 | 70.4142 | 0.01 | −0.03 | Deeply weathered sandstone | Small underground storage room |
| DUD | 23.3195 | 70.1270 | −0.03 | +0.06 | ?? | Ground floor of damaged one-story masonry |
| KHA | 23.4605 | 70.3517 | 0.02 | 0.27 | Deeply weathered sandstone | Ground floor of damaged one-story masonry |
| LBR | 23.9875 | 69.7463 | −0.27 | −0.05 | Slightly indurated sediments | Free field |
| LIQ | 23.4875 | 69.9162 | 0.13 | 0.98 | Deep unconsolidated sediment | Free field |
| LOT | 23.2383 | 69.6727 | 0.01 | 0.11 | Thin soil over sandstone | Basement of two-story stone house |
| VER | 23.8888 | 70.4138 | −0.05 | −0.02 | Sandstone | Thatch hut |

tion terms in the locations. Station corrections based on average travel-time residuals at each station are shown in Table 1. The mean location root mean square (rms) travel-time error was 0.035 sec with a standard deviation of 0.02 sec.

To date, we have located 1243 aftershocks recorded by our temporary network. Although incomplete, the analysis reveals major features of the aftershock distribution during the deployment. Additional aftershock locations derived from our data set are unlikely to dispel our conclusions, particularly since we have concentrated on the most well recorded events.

## Aftershock Locations

Figure 2 summarizes the main features of the observed aftershock distribution, which we report in this article. Corroborative evidence and finer details may be seen by examining the locations. (Ⓔ A table containing the source parameters of recorded Bhuj aftershocks is available online at the SSA Web site.) Aftershocks were distributed over a fairly broad area, but most epicenters fell within a roughly trapezoidal shape with parallel sides that strike nearly east–west. The northern edge near 23.6° is the longest (about 55 km) and 5–10 km deep. The southern edge near 23.3° is approximately 25 km long and ~35 km deep. In cross section a dipping concentration of aftershocks extends from between 5 and 10 km to about 35 km deep (cross section AB in Fig. 2). The Moho in the region is believed to lie at 40 km; thus the aftershocks extended from upper crust nearly, perhaps completely, through the crust. Although it is not well displayed in Figure 2, aftershocks were more concentrated along the southern, eastern, and western edges of the trapezoid and were more sparse in the middle portion. Mainshock hypocentral location estimates (USGS: 23.36° N, 70.34° E, $H$ = 22 km; IMD: 23.40° N, 70.28° E, $H$ = 25 km) are near the southern edge of the trapezoid, and teleseismically determined mainshock focal mechanisms generally yield an approximately south-dipping nodal plane (Wesnousky *et al.*, 2001; Antolik and Dreger, 2003). We conclude that the south-dipping aftershocks highlight the mainshock rupture: trapezoidal in shape and extending into the deep crust.

At its western edge, the aftershock distribution was truncated abruptly, as if the mainshock rupture was stopped by a sharp discontinuity. The eastern part of the aftershock swarm is more complicated. A concentration of aftershocks appears to define (albeit indistinctly) another smaller plane

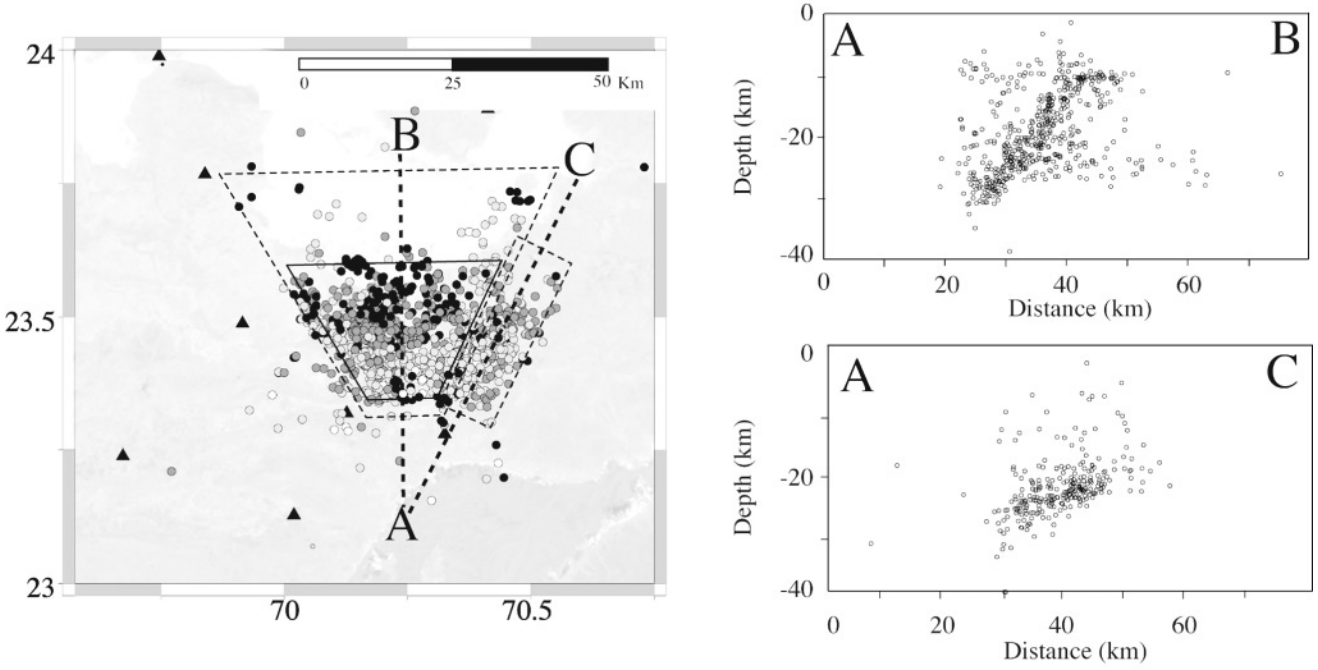


Figure 2. Bhuj aftershock locations. On the map at the left we plot 887 aftershock epicenters over a satellite image. These locations represent events with depth errors less than ±3 km and horizontal uncertainties less than ±2 km. The mean rms travel-time uncertainty for these data is 0.0036 sec, and the greatest rms uncertainty is 0.01 sec. Epicenters are shaded by depth, with white >30 km, light gray 20–30 km, dark gray 10–20 km, and black <10 km. Small black triangles are seismograph sites. The dashed quadrilaterals show spatial regions for events shown in the cross sections at right. The solid trapezoid is the surface projection of the rupture model discussed in text. (Ⓔ A table containing the source parameters of recorded Bhuj aftershocks is available online at the SSA Web site.)

(cross section AC in Fig. 2). This eastern plane is about 5 km wide and 10–15 km long and dips to the west or southwest at a much lower angle (~20°–30°) than the larger plane. This smaller eastern plane merges with the south-dipping plane at its deep southern edge. We interpret this plane as a separate rupture, perhaps slipping during the mainshock, or perhaps during an early, large aftershock.

Although the aftershocks were close to the Kachchh Mainland and Wagad faults, both faults are too far south to have hosted the mainshock. The aftershocks were well south of the Island Belt fault, east of the Banni fault, and for the most part north of the surface trace of the Kachchh Mainland fault and the Wagad fault. Earthquakes occurring outside the trapezoid were, we assume, not on the mainshock fault plane.

Another feature worthy of mention (although we do not have a ready explanation for it) is a narrow, rather sparse, clustering of aftershocks that trend north–northeast (Fig. 2; longitude 70.4°–70.5°, latitude 23.6°–23.75°). These are fairly deep (~25 km) and may highlight a feature in the footwall block of the main plane that plunges gently to the north.

The aftershock locations we report are consistent with rupture during the mainshock of a fault that was not previously mapped and that does not reach the surface as a major topographic feature. Based on geology and topography alone, it would have been very difficult to foresee the blind reverse rupture that was the Bhuj earthquake. While the epicenter may have been close to the Kachchh Mainland and Wagad faults (Fig. 1), the base of the rupture lies under the surface trace of these faults, and the dip of the aftershock plane is such that if it extended to the surface, the rupture would probably have done so in the southern part of the Great Rann; field investigations there failed to reveal any primary surface faulting from the Bhuj earthquake (Wesnousky *et al.*, 2001). We have calculated the expected surface deformation pattern from the rupture model we propose, which featured as much as 3 m of surface uplift south of the projected intersection of the rupture plane with the surface. If ruptures similar to that which produced the Bhuj earthquake had recurred frequently, one might expect to see a clear topographic expression of the faulting. There is not. Thus we conclude that the Bhuj earthquake, if a recurrent event, represents either a very slowly slipping or a very newly active fault.

The relative abundance of aftershocks around the edge of the south-dipping trapezoidal plane may reflect an increase in stress around the edges of a high-slip patch (e.g., Kanamori, 1994; Antolik and Dreger, 2003). Hypocenter estimates from regional and teleseismic observations are, within plausible uncertainties, also consistent with a rupture that initiated within the trapezoidal rupture area suggested by the aftershocks. The duration of rupture, as reflected by the STF (Ruff and Miller, 1994; Ruff, 2001; Antolik and Dreger, 2003; Singh *et al.*, 2003) was relatively short and simple for an earthquake of this magnitude. Taken together, these observations suggest that the Bhuj rupture was very powerful, with seismic energy being released quickly and from a small crustal volume, that is, a relatively high stress drop (both static and dynamic) earthquake. However, recent results by Singh *et al.* (2003) suggest that the rupture featured low seismic efficiency and apparent stress, despite its rather high static stress drop. Singh *et al.* suggested that although the rupture took place under great stress, some mechanism operated to reduce the energy available for seismic radiation; for example, the rupture expended energy breaking fresh rock or in rapid ductile deformation of deep crustal rocks.

*Inferences from Depth Distribution.* Bhuj aftershocks were surprisingly deep. The depth distribution of aftershocks (Fig. 3) reveals that the most probable depth for a Bhuj aftershock was in the lower crust at about 26 km deep. Moreover, the depth distribution was bimodal, with another smaller peak in aftershock production in the upper crust at about 10 km. In order to test the robustness of this observation to assumptions made in the inversion process, we relocated the aftershocks using a range of different velocity models and starting depths for the inversion. While details

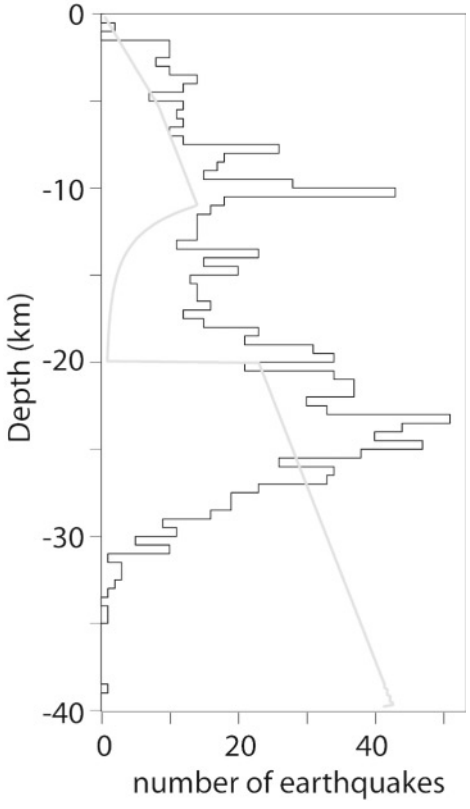


Figure 3. Depth distribution of Bhuj aftershocks shown on Figure 2. The gray line shows model of crustal strength envelope for two-layer crust (granite over diabase at 20 km) with 60 mW/m$^2$ heat flow and low internal heat production, under a contractional strain rate of $10^{-12}$/yr.

of the aftershock distributions resulting from these perturbations were altered, the bimodal distributions of depths, including most of the earthquakes locating in the lower crust, remained a robust feature.

As to whether the deep seismicity we observed is characteristic of the region, or represents some perturbed brittle failure conditions in the aftermath of the Bhuj mainshock, we cannot say. We do note that many of the aftershocks that located rather far from the putative main rupture plane (Fig. 2) clearly also were deep within the lower crust. This suggests to us that the lower crust in the Kachchh region is generally brittle and that the aftershocks do not necessarily represent a perturbed failure criterion.

Not only were aftershocks clearly nucleating nearly to the Moho, but also the observations are consistent with deep slip during the mainshock. These observations are at odds with the conclusions of several earlier, and widely cited, studies. Chen and Molnar (1983), for example, concluded that the evidence for deep crustal ruptures in continental interiors is scant. The three variables that are thought to dominate the brittle strength of crustal rocks are the lithology, the temperature, and the strain rate. If a crust is dominantly composed of quartz-rich rocks, for a wide range of temperature profiles a single brittle–ductile transition (BDT) is expected. Above the BDT deformation is by brittle failure, while beneath it deformation is dominated by transition to fully plastic flow. The BDT is the cutoff depth generally observed for shallow earthquakes. If the rocks are dominantly mafic (as in oceanic lithosphere), then the BDT will be deeper, because mafic minerals are generally more brittle at the same temperature than acidic minerals (e.g., Scholz, 1990). However, if the crustal lithology is layered, with mafic materials underneath acidic rocks, then more BDTs are possible, depending on the temperature profile. Increasing temperature inhibits brittle failure, and a steeper temperature lapse rate (higher heat flow) raises the BDT. All other variables held constant, brittle behavior is enhanced by high strain rate. Therefore, if a rock under environmental conditions in which it would be expected to deform in a ductile mode experiences a sudden rapid increase in strain rate, it might possibly become brittle. However, since interseismic (ductile) deformation would presumably decrease stress in the midcrust to levels lower than required for brittle failure, any increase in strain rate would have to be associated with an increase in stress sufficient to drive brittle failure.

In light of these models, we suggest alternative interpretations of the bimodal depth distribution. The first, and our preferred, hypothesis is that the distribution mirrors a similar bimodal depth-dependent brittle strength profile for thrust faulting (Fig. 3; e.g., Manglik and Singh, 1999). A bimodal brittle strength profile would be expected for a layered lithology with quartz-rich upper crust and a more mafic lower crust ($>$20 km), assuming a suitable temperature profile. Our data collection period was too brief to rule out the possibility that brittleness in the lower crust was a temporary feature, with brittle strength enhanced by rapid strain rate during early postseismic viscoelastic strains (e.g., Johnston *et al.*, 2001). However, the diffuse deep crustal earthquakes we observed at large distances from the rupture were far enough away that post-mainshock strain rates would probably have been quite low. An alternative hypothesis for the bimodal depth distribution is that the relative lack of abundance of aftershocks between $\sim$12 and 20 km deep reflects the fact that most of the slip during the mainshock took place in this depth range and that less stress remained in the rocks after the mainshock rupture to drive aftershocks (Antolik and Dreger, 2003). This hypothesis implies a single crustal brittle rheology with a BDT at about 26 km and a broad transition to fully plastic flow somewhere below about 35 km. We prefer the layered rheological explanation for the aftershock observations because of the observations of deep earthquakes remote from the apparent rupture plane. A layered lithology in the Kachchh rift is also consistent with models of continental rifting that feature the emplacement of a rift pillow (i.e., Hildenbrand *et al.*, 1992), mafic intrusions, or underplating associated with crustal thinning during the rifting process. This explanation is also consistent with observations of deep crustal seismicity from other failed continental rifts (e.g., Nyblade and Langston, 1995; Zoback and Richardson, 1996; Singh *et al.*, 1999b).

Even within India, the Kachchh rift is not the only intraplate region to experience deep earthquakes (e.g., Rao *et al.*, 2002). The Shillong plateau, a region bounded by shallow crustal faults in India (one of which is thought to have caused the great Assam earthquake of 1897, the last large continental intraplate earthquake [Bilham and Gaur, 2000]) experiences upper-mantle earthquakes (e.g., Chen and Molnar, 1983). And the 1997 Jabalpur earthquake originated at a depth of $\sim$35 km (Singh *et al.*, 1999b). Both of these areas are located within a system of rifts that cross the Indian shield. Taking a wider view, east Africa experiences deep crustal earthquakes (Nyblade and Langston, 1995) in rocks presumably once adjacent to those that now constitute Kachchh crust. Nyblade and Langston (1995) concluded that a combination of mafic lower crust and lower temperatures than expected from surface heat flow measurements must be invoked to explain brittle behavior of deep crustal rocks in east Africa. While there are few published heat flow measurements in Kachchh, Roy (2003) noted a somewhat higher than normal heat flow from the Bhuj earthquake source region (55–93 mW/m$^2$), which suggests higher rather than lower deep-crust temperatures unless heat production is unusually high in shallow rocks.

Therefore, while not definitive, the occurrence of deep Bhuj aftershocks provides strong support for the presence of relatively cold mafic rocks in the deep crust. Taken with other observations, we suggest that this may provide a more general condition for seismogenesis in old rift structures. Johnston *et al.* (1994) noted that all known large ($M \geq 7$) stable continental intraplate earthquakes have taken place not in shields, but rather in areas that have been subject to rifting at some time since the Proterozoic.

*Focal Mechanisms.* We determined focal mechanisms from first motions for ~500 aftershocks. The azimuthal coverage was not always very good, and station density was low, so the fault-plane solutions have large uncertainties. However, given the large number of aftershocks, and the broad distribution of aftershocks with respect to the network station distribution, we may use the results to state a first-order conclusion. Examining the distribution of *P* and *T* axes (Fig. 4) reveals a variety of focal mechanisms and that, taken as a whole, the ensemble is consistent with north–south directed contraction and reverse slip on roughly east–west–striking planes. Waveform modeling studies should enable us better moment tensor determinations so that we may make more detailed comparisons with the aftershock location patterns.

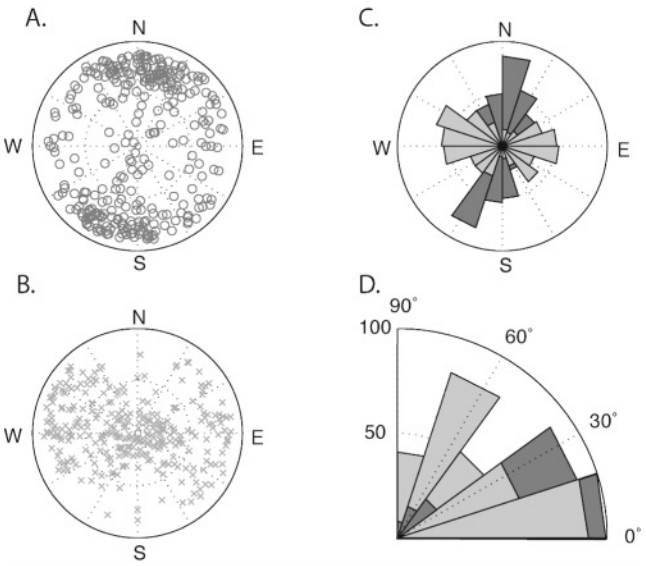


Figure 4. *P* and *T* axes of Bhuj aftershock focal mechanisms. (A) Stereoplot of *P*-axis orientations; (B) stereoplot of *T*-axis orientations; (C) rose diagram of *P*- (dark shading) and *T*-axis (light shading) azimuths; (D) distribution of plunges of *P* (dark shading) and *T* axes (light shading).

## Interpretations

We used the fault geometry revealed by the aftershocks together with the teleseismically determined scalar seismic moment to estimate the static stress drop. For the calculation, we assume that the mainshock ruptured a trapezoidal patch 50 km at its widest (up-dip) edge buried 10 km, extending over 35 km down-dip to a depth of 35 km, and tapering to an along-strike length at the deep side to 25 km. The area of this trapezoid is roughly 1350 km$^2$. Because the geometry of the fault is not one of those for which an analytical expression relating stress-drop and fault slip exists, we use a boundary-element model (Gomberg and Ellis, 1994) to drive a freely slipping trapezoidal fault with the geometry assumed for the Bhuj mainshock. We apply a regional load such that the average slip $D$ on the fault of area $A$ is that needed to match the scalar seismic moment $M_0$:

$$M_0 = \mu DA,$$

where $\mu$ is the modulus of rigidity, which for the Kachchh lower crustal rock we take to be (4–4.5) $\times$ $10^{11}$ dyne cm$^2$. Estimates for $M_0$ from teleseismic data varied in the range of (2.3–3.6) $\times$ $10^{20}$ N m (e.g., Wesnousky *et al.*, 2001), and we obtain $A$ varying from ~1200 to 1500 km$^2$ based on our aftershock distributions. The stress drop is the shear stress resolved on the rupture plane that best matches the averages slip needed to satisfy equation (1). Given the range of estimates for $M_0$, $\mu$, and uncertainties in $A$, our estimates of static stress drop range from ~120 to ~180 bars, with a preferred estimate of 160 bars. A circular fault having the same area would give a static stress drop of 170 bars. This compares with an estimate of static stress drop derived from finite fault inversion of teleseismic data of ~20 MPa (Antolik and Dreger, 2003).

The abrupt termination of aftershocks along a northwest trend at the western edge of the rupture appears as if the rupture at this edge may have ran up against a near-vertical structure here. There is no fault mapped here, although the boundary roughly coincides with the edge of the Banni Plain and Great Rann landscapes (Figs. 1 and 2). The complexities at the eastern edge of the aftershocks as they terminate near the Wagad uplift/Great Rann boundary also suggest a rupture running into a geometric barrier at this edge. Taking the teleseismic studies together with our aftershock distributions, one can propose a scenario for the mainshock rupture. The rupture appears to have nucleated near the center of the aftershock cluster, at midcrustal depth (>20 km), spread quickly, with high stress drop but low seismic efficiency, both along strike and up- and down-dip. Laterally it spread until it encountered sufficient structural heterogeneity to abruptly stop the powerful rupture. Down-dip it penetrated through the lower crust, but diminishing in length (either because of interfering structures or due to dynamical effects related to rupturing deep-crustal rocks). Up-dip the rupture propagated until it reached a depth of 10 km, or perhaps 5 km, but did not make it to the surface. We hypothesize that in the shallow crust (<10 km or so), similar to the situation at the east and western edges, there were no appropriately oriented structures to continue the rupture.

Overall, the Bhuj earthquake appears to have been a blind reverse earthquake, rupturing a fault that has been reactivated within the currently applied tectonic load, north–south compression within the Indian plate resulting from the collision of India with Eurasia. However, the fault dipped so steeply that it must be classified as nearly a severely misoriented fault (Sibson and Xie, 1998). The mainshock ruptures apparent steeply dip, and evidence of deep crustal seismogenesis is consistent with suggestions that elevated fluid pressures may weaken such faults. It is difficult to conceive of free water in faults down to 35 km, and it seems much

more likely that any fluid involved would be something more exotic, such as carbon dioxide.

Moreover, due to (probably) slow deformation rates and low overall slip amounts within the plate interior, large through-going faults may not have developed. The mapped surface faults, while prominent topographically, may not represent the relevant active seismic hazard in Kachchh. Moreover, the small rupture area of the Bhuj rupture makes it clear that the earthquake did not relieve stress throughout the region. Although the history of large earthquakes in the region is not well known, it is likely that significant regions of high stress remain to drive future earthquakes, particularly between the 1819 and 2001 ruptures.

The duration of our aftershock study was not long compared to the aftershock sequence itself. Even within the 3-week duration of our study, aftershock production seemed to decrease only slightly and even increased following the occurrence of two large aftershocks ($M \sim 5$) on 19 February. These aftershocks were the largest during our deployment. However, aftershock observations produced by the IMD from regional data suggest that there were fewer large aftershocks than might be expected from an $M$ 7.6 earthquake. The largest aftershock ($M \sim 6$) occurred within 1 day. Fewer than 10 aftershocks with $M > 5$ took place in the year following the mainshock, and these were all within the first month, despite a fairly rich production of small-magnitude earthquakes that has continued at least through the summer of 2003 (P. Mandal, personal comm., 2003; J. Zollweg, personal comm., 2003).

## Bhuj: A Typical Large Continental Intraplate Earthquake?

Our interest in the Bhuj earthquake was initially stimulated because the region shares characteristics with the New Madrid seismic zones. This intraplate North American active seismic zone also lies within Precambrian cratonic basement, topped by relatively thin Paleozoic and younger sediments, including thick (~1 km) unconsolidated Cenozoic and Holocene sediments at the surface. Both regions have experienced recurrent and failed rifting but are currently being compressed. The calculated seismic hazard in both regions is dominated by the recurrence of large earthquakes with the previous occurrences in the nineteenth century. There are differences, too, between the Bhuj and New Madrid areas, and future work will need to explore the extent to which the Bhuj earthquake may be analogous to the New Madrid region seismicity (Ellis *et al.*, 2001).

The aftershock studies are consistent with an interpretation that the Bhuj earthquake was a blind reverse rupture, to considerable depth, of a fault internal to an old failed continental rift zone. The largest such earthquake recorded by modern seismic instrumentation, Bhuj was fairly high in stress drop, and powerful. It ruptured a previously unmapped fault, which was not evident at the surface. From the perspective of spatial aftershock distributions, several tantalizing features are apparent beside the main rupture plane itself, which future investigations may clarify. These include hints at small active structures, perhaps aftershocks of aftershocks, or maybe intersecting structures slipping sympathetically during the mainshock.

## Acknowledgments

Acquisition of Bhuj aftershock data reflects the effort and support of many individuals and groups; Kirit Budhbatti and officials of the state of Gujarat deserve particular gratitude. This work was supported in part by the Mid-America Earthquake Center through the Earthquake Engineering Research Centers Program of the National Science Foundation under NSF Award Number EEC-9701785. Any opinions, findings, and conclusions or recommendations expressed in this material are those of the author(s) and do not necessarily reflect those of the National Science Foundation. Transportation and customs formalities were facilitated by FedEx corporation and by G. Patterson. J. Bollwerk and P. Rydelek provided valuable field assistance; G. Steiner, C. McGoldrick, and M. Withers assistance in the laboratory. The manuscript received careful and useful reviews by K. Rajendran and S. K. Singh. This is CERI Contribution Number 474.

## References

Antolik, M., and D. S. Dreger (2003). Rupture process of the 26 January 2001 $M_w$ 7.6 Bhuj, India, earthquake from teleseismic broadband data, *Bull. Seism. Soc. Am.* **93,** 1235–1248.

Beck, R. A., D. W. Burbank, W. J. Sercombe, G. W. Riley, J. K. Barndt, J. R. Berry, J. Afzal, A. M. Khan, H. Jurgen, J. Metje, A. Cheema, N. A. Shafique, R. D. Lawrence, and M. A. Khan (1995). Stratigraphic evidence for an early collision between India and Asia, *Nature* **373,** 55–58.

Bendick, R., R. Bilham, E. Fielding, V. K. Gaur, S. E. Hough, G. Kier, M. N. Kukarni, S. Marin, K. Mueller, and M. Mukul (2001). The 26 January 2001 "Republic Day" earthquake, India, *Seism. Res. Lett.* **72,** 328–335.

Besse, J., V. Courtillot, J. P. Pozzi, M. Westphal, and Y. X. Zhou (1984). Paleomagnetic estimates of crustal shortening in the Himalayan thrusts and Zangbo suture, *Nature* **311,** 621–626.

Bilham, R., and V. K. Gaur (2000). The geodetic contribution to Indian seismotectonics, *Curr. Sci.* **79,** 1259–1269.

Bilham, R., K. Wallace, V. Gaur, R. Bendick, G. Kier, and F. Blume (2002). Geodetic constraint of the $M = 7.6$ Bhuj 2001 rupture and convergence across the Rann of Kachchh 1856–2001. *EOS* **83,** no. 47, (Fall Meet. Suppl.).

Biswas, S. K. (1980). Structure of Kutch–Kathiawar Region, W. India, in *Proc. 3rd Indian Geological Congress*, Pune, India, 23–27 November 1980, 255–272.

Biswas, S. K. (1981). Basin framework, palaeoenvironment, and depositional history of the Mesozoic sediments of Kutch Basin, western India, *Q. J. Geol. Min. Met. Soc. India* **53,** no. 1–2, 56–85.

Biswas, S. K. (1982). Rift basins in the western margin of India and their hydrocarbon prospects with special reference to Kutch basin, *Am. Assoc. Petrol. Geol. Bull.* **66,** 1497–1513.

Biswas, S. K. (1987). Regional tectonic framework, structure, and evolution of the western marginal basins of India, *Tectonophysics* **135,** 307–327.

Centroid Moment Tensor (CMT) Catalog, www.seismology.harvard.edu/CMTsearch.html (last accessed April 2004).

Chen, W.-P. and P. Molnar (1983). Focal depths of intracontinental and intraplate earthquakes and their implications for the thermal and mechanical properties of the lithosphere, *J. Geophys. Res.* **88,** 4183–4214.

Chung, W. Y., and H. Gao (1995). Source parameters of the Anjar earth-

quake of July 21, 1956, India, and its seismotectonic implications for the Kutch rift basin, *Tectonophysics* **242,** 281–292.

Courtillot, V., J. Besse, D. Vandamme, R. Montigny, J. J. Jaeger, and H. Cappetta (1986). Deccan flood basalts at the Cretaceous/Tertiary boundary? *Earth Planet. Sci. Lett.* **80,** 361–374.

Ellis, M., J. Gombeg, and E. Schweig (2001). India earthquake may serve as analog for New Madrid earthquakes, *EOS* **82,** no. 32, 345–350.

Gomberg, J., and M. Ellis (1994). Topography and tectonics of the central New Madrid seismic zone: results of numerical experiments using a three-dimensional boundary element program. *J. Geophys. Res.* **99,** 20,299–29,310.

Gowd, T., A. S. Rao, and V. Gaur (1992). Tectonic stress field in the Indian subcontinent, *J. Geophys. Res.* **97,** 11,879–11,888.

Hildenbrand, T. G., J. G. Rosenbaum, and R. L. Reynolds (1992). High-resolution aeromagnetic study of the New Madrid seismic zone: a preliminary report, *Seism. Res. Lett.* **63,** 209–222.

Horton, S., P. Bodin, and M. Withers (2001). Aftershock measurements, in *The Bhuj Earthquake of 2001*, D. Abrams, M. Ascheim, P. Bodin, S. Deaton, S. Dotson, D. Frost, S. K. Gosh, S. Horton, A. Johnston, J. Nichols, T. Rosetto, M. Tuttle, and M. Withers (Editors), Mid-America Earthquake Center, CD Series 01–04, 11–18.

Hough, S. E., S. Martin, R. Bilham, and G. M. Atkinson (2002). The 26 January 2001 *M* 7.6 Bhuj, India earthquake: observed and predicted ground motions, *Bull. Seism. Soc. Am.* **92,** 2061–2079.

Jaeger, J.-J., V. Courtillot, and P. Tapponnier (1989). Paleontological view of the ages of the Deccan Traps, the Cretaceous/Tertiary boundary, and the India–Asia collision, *Geology* **17,** 316–319.

Johnston, A. C., P. Bodin, and P. A. Rydelek (2001). The Republic Day earthquake: An explanation for deep aftershocks in the ductile lower crust, *Seism. Res. Lett.* **72,** 397–398.

Johnston, A. C., K. J. Coppersmith, L. R. Kanter, and C. A. Cornell (1994). Assessment of Large Earthquake Potential, in The Earthquakes of Stable Continental Regions, Vol. 1, Electric Power Research Institute, Palo Alto, California.

Kanamori, H. (1994). Mechanics of earthquakes. *Ann. Rev. Earth Planetary Sci.* **22,** 207–237.

Lahr, J. C. (1999). HYPOELLIPSE: a computer program for determining local earthquake hypocentral parameters, magnitude, and first-motion pattern (Y2K compliant version), *U.S. Geol. Surv. Open-File Rept. 99–23*.

Malik, J. N., P. S. Sohoni, R. V. Karanth, and S. S. Merh (1999). Modern and historic seismicity of Kachchh Peninsula, Western India, *J. Geol. Soc. India* **54,** 545–550.

Malik, J. N., P. S. Sohoni, S. S. Merh, and R. V. Karanth (2000). Palaeoseismology and neotectonism of Kachchh, western India, in *Active Fault Research for the New Millennium*, K. Okumura, H. Goto, and K. Takada (Editors), Proc. of the Hokudan International Symposium and School on Active Faulting, 251–259.

Manglik, A., and R. N. Singh (1999). Rheological stratification of the Indian continental lithosphere: role of diffusion creep, *Proc. Indian Acad. Sci. Earth Planet. Sci.* **108,** 15–21.

Negishi, H., J. Mori, T. Sato, R. Singh, S. Kumar, and N. Hirata (2002). Size and orientation of the fault plane for the 2001 Gujarat, India earthquake ($M_w$ 7.7) from aftershock observations: a high stress drop event, *Geophys. Res. Lett.* **29,** 1949, doi 10.1029/2002GL015280.

Nyblade, A. A., and C. A. Langston (1995). East African earthquakes below 20 km depth and their implications for crustal structure, *Geophys. J. Int.* **121,** 49–62.

Patriat, P., and J. Achache (1984). India–Eurasia collision chronology has implications for crustal shortening and driving mechanism of plates, *Nature* **311,** 615–621.

Rajendran, C. P., and K. Rajendran (2001). Deformation characteristics and past seismicity associated with Kuch seismic zone, *Bull. Seism. Soc. Am.* **91,** 407–426.

Rao, N. P., T. Tsukuda, M. Kosuga, S. C. Bhatia, and G. Suresh (2002). Deep lower crustal earthquakes in central India: inferences from analysis of regional broadband data of the 1997 May 21, Jabalpur earthquake, *Geophys. J. Int.*, **148,** 132–139.

Roy, A. B. (2003). Geological and geophysical manifestations of the Reunion plume–Indian lithosphere interactions: evidence from northwest India, *Gondwana Res.* **6,** 487–500.

Ruff, L. (2001). Source Time Function online catalog, www.geo.lsa.umich.edu/SeismoObs/STF/010126_India (last accessed April 2004).

Ruff, L. J., and A. D. Miller (1994). Rupture process of large earthquakes in the northern Mexico subduction zone, *Pageoph* **142,** 101–172.

Scholz, C. H. (1990). *The Mechanics of Earthquakes and Faulting*, Cambridge U Press, New York, 439 pp.

Sibson, R. H., and G. Xie (1998). Dip range for intracontinental reverse fault ruptures: truth not stranger than fiction? *Bull. Seism. Soc. Am.* **88,** 1014–1022.

Singh, P. (1995). Calcareous nanoplankton biostratigraphy of the subsurface Jurassic strata of Banni Rann, Kachchh, Gujarat, India, *Geosci. J.* **16,** 19–37.

Singh, S. K., M. Ordaz, R. S. Dattatrayam, and H. K. Gupta (1999a). A spectral analysis of the May 21, 1997 Jabalpur, India earthquake ($M_w$ = 5.8) and estimation of ground motion from future earthquakes in the Indian shield region, *Bull. Seism. Soc. Am.* **89,** 1620–1630.

Singh, S. K., R. S. Dattatrayam, N. M. Shapiro, P. Mandal, J. F. Pacheco, and R. K. Midha (1999b). Crustal structure and upper mantle structure of peninsular India and source parameters of the May 21, 1987, Jabalpur earthquake ($M_w$ = 5.8): results from a new regional broadband network, *Bull. Seism. Soc. Am.* **89,** 1631–1641.

Singh, S. K., J. F. Pacheco, B. K. Bansall, X. Pérez-Campos, R. S. Dattatrayam, and G. Suresh (2003). A source study of Bhuj, India, earthquake of 26 January, 2001 ($M_w$ 7.6), in *Proc. of the Indo–US Workshop on Seismicity and Geodynamics*, National Geophysical Research Institutue, Hyderabad, India, 6–10 October 2003, 130 pp.

Siveright, R. (1907). Cutch and the Ran, *Geographical J.* **24,** 518–539.

Talwani, P., and A. Gangopadhyay (2001). Tectonic framework of the Kachchh earthquake of 26 January 2001, *Seism. Res. Lett.* **72,** 336–345.

Wesnousky, S. G., L. Seeber, T. K. Rockwell, V. Thakur, R. Briggs, S. Kumar, and D. Ragona (2001). Eight days in Bhuj: field report bearing on surface rupture and genesis of the January 26, 2001 Republic Day earthquake of India, *Seism. Res. Lett.* **72,** 514–524.

Zoback, M. L., and R. M. Richardson (1996). Stress perturbation associated with the Amazonas and other ancient continental rifts, *J. Geophys. Res.* **101,** 5459–5476.

Center for Earthquake Research and Information
University of Memphis
Memphis, Tennessee 38152
bodin@ceri.memphis.edu

Manuscript received 20 August 2003.